Low-concentration NO_x removal using plasma-chemical hybrid process combined with limestone-gypsum desulfurization

Takeru Itagaki[1], Junta Inoue[1], Tomoyuki Kuroki[1, *], Haruhiko Yamasaki[1], Hashira Yamamoto[2], Masanori Hattori[3], Masaaki Okubo[1]

[1] Department of Mechanical Engineering, Osaka Metropolitan University, Japan
[2] Nihon Yamamura Glass Co., Ltd., Japan
[3] Chubu Electric Power Co., Inc., Japan

* Corresponding author: kuroki@omu.ac.jp (Tomoyuki Kuroki)

Abstract

Nitrogen oxides (NO_x) and sulfur oxides (SO_x) emitted from thermal power plants are hazardous pollutants causing acid rain and air pollution. To meet the respective emission regulations, NO_x is treated using the selective catalytic reduction (SCR) method, while SO_x is treated using the lime gypsum method before being discharged via a flue-gas stack. Recently, some local governments and companies have signed environmental protection agreements that impose stricter limits than national emission regulations. Moreover, existing technologies, such as low-NO_x burners and SCR, exhibit limitations in achieving further NO_x reduction. Therefore, further pollutant reduction measures are required, particularly NO_x treatment methods that can be retrofitted into existing flue gas treatment systems in thermal power plants. A plasma-chemical hybrid process (PCHP) offers a promising solution for simultaneous removal of NO_x and SO_x and can be retrofitted. In this study, laboratory-scale experiments were conducted to evaluate the simultaneous removal of low-concentration NO_x and high-concentration SO_x using ozone (O_3) injection and absorption towers, simulating the integration of PCHP into the absorption tower of flue gas treatment equipment in a coal-fired power plant. The results show that PCHP enables simultaneous removal of low-concentration NO_x and high-concentration SO_2, although water spray impacts NO oxidation.
.

Keywords: Low-concentration NO_x, plasma-chemical hybrid process, SO_x, limestone-gypsum desulfurization.

1. Introduction

In recent years, the demand to reduce carbon dioxide (CO_2) emissions, a major contributor to global warming, has led to the consideration of large-scale renewable energy integration into power generation [1–5]. However, the power output from renewable energy sources fluctuates depending on the time and weather conditions, resulting in significant unstable electricity supply. Therefore, it is necessary to stabilize the power supply with thermal power generation, which can readily adjust electricity output [4, 5]. Nitrogen oxides (NO_x) and sulfur oxides (SO_x) emitted from thermal power plants are hazardous pollutants causing acid rain and air pollution. Their emissions are regulated under air pollution control laws [6]. For these emissions, NO_x is treated using the selective catalytic reduction (SCR) method [6–11], and SO_x is treated using the lime gypsum method [12–14] to meet the respective emission regulations. Recently, some local governments and companies have signed environmental protection agreements that impose stricter limits than the national emission regulations, requiring further pollutants reduction. However, existing technologies, such as low-NO_x burners and SCR, have limitations in achieving further NO_x reduction. Additionally, the anticipated large-scale introduction of renewable energy will require thermal power plants to readily adjust the electricity output, resulting in reduced NO_x emissions. Therefore, there is a need for NO_x treatment methods that can be retrofitted into the existing flue gas treatment facilities in thermal power plants.
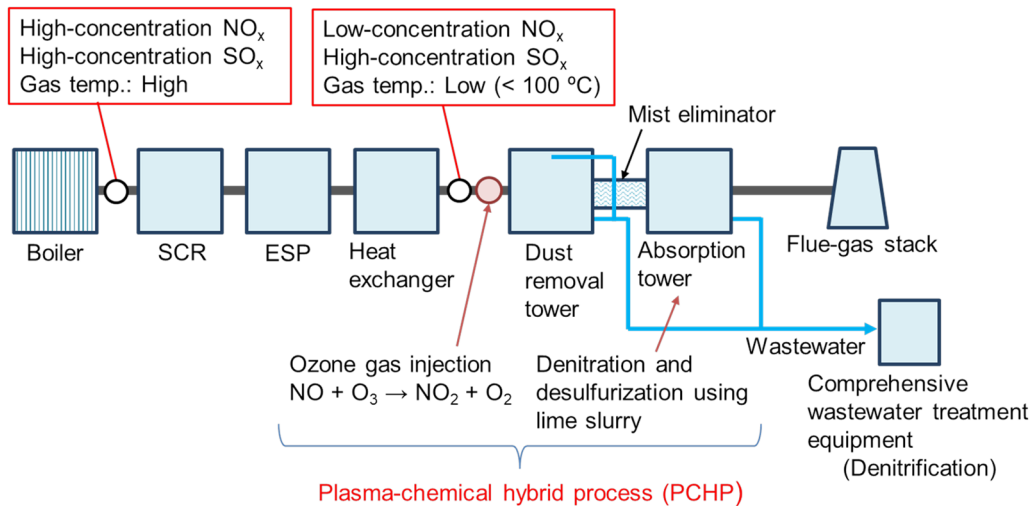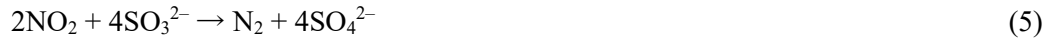
Fig. 1. Flue gas treatment flow in thermal power plant after the introduction of PCHP.

Many energy-saving and highly efficient NO_x treatment methods using atmospheric pressure and low-temperature plasma have been reported [6, 15–18]. Previous studies have shown that the plasma chemical hybrid process (PCHP) technology, which combines a plasma method for oxidizing nitric oxide (NO) in boiler flue gas to nitrogen dioxide (NO_2) a subsequent reaction process for reducing and removing NO_2 produced through oxidation using sodium sulfite (Na_2SO_3) solution, can achieve highly efficient treatment [19–18]. If NO_2 can be removed using calcium sulfite ($CaSO_3$), which is produced by the reaction between a calcium carbonate ($CaCO_3$) slurry and SO_x, it could be used in the flue gas treatment systems of coal-fired power plants [19–24]. Fig. 1 shows the flue gas flow in a coal-fired power plant after introducing PCHP. Typically, NO_x treatment is first performed on flue gas from a boiler in the denitration equipment at a coal-fired power plant. The gas is then cooled in a heat exchanger, dust is removed in a dust removal tower, passed through a mist removal system, and then subjected to SO_x treatment in an absorption tower, where a $CaCO_3$ slurry is used to remove not only SO_x but also NO_x, and simultaneous removal of NO_x and SO_x is achieved. PCHP has been applied to glass melting furnaces, efficiently treating NO_x and SO_x [23–25]. The reaction of O_3 with SO_2 (reaction rate constant $k = 1.92 \times 10^{-22}$ cm^3 molecule^{-1}s^{-1}, 25 °C) is much slower than its reaction with NO ($k = 1.7 \times 10^{-14}$ cm^3 molecule^{-1}s^{-1}, 25 °C). Consequently, O_3 selectively oxidizes NO [25–27], with no effect of SO_x on NO oxidation observed for glass melting furnace exhaust gases containing equal amounts of NO_x and SO_x [23, 24]. However, as shown in Fig. 1, when PCHP is introduced, high concentrations of SO_x are present relative to low concentrations of NO_x, SO_2 may have inhibited NO oxidation, resulting in inadequate NO_x treatment. In addition, it is necessary to investigate the performance of O_3 oxidation by water spraying, because O_3 injection involves spraying with a two-fluid nozzle to diffuse O_3 into the flue gas. To evaluate the NO oxidation performance in the presence of low-concentrations of NO_x and high-concentrations of SO_2, NO oxidation experiments were conducted using an O_3 injection tower. Furthermore, we evaluated the simultaneous removal of NO_x and SO_2 by combining O_3 injection under water spray conditions in the O_3 injection tower and $CaCO_3$ slurry injection in the absorption tower, assuming that the PCHP was introduced into the dust removal and absorption towers in the flue gas treatment flow of a coal-fired power plant. In previous simultaneous NO_x and SO_x removal experiments using PCHP, O_3 was injected at the same concentration as NO, and sufficient NO oxidation and NO_x treatment were achieved [23, 24]. However, when PCHP is introduced at low NO_x concentrations, the O_3 concentration is also low, making it susceptible to the inhibition of oxidation by the water spray. Therefore, we evaluated the appropriate O_3 concentration for low-concentration NO_x treatment to improve removal efficiency.

2. Chemical reactions in PHCP

When PCHP is integrated into flue gas treatment in thermal power plants, NO in the flue gas is oxidized by O_3 to form NO_2 during the plasma process. During the chemical process, SO_2 and NO_2 are absorbed by the $CaCO_3$ slurry, resulting in desulfurization and denitrification. When CO_2 is included in the simulated flue gas, the

reaction of the $CaCO_3$ slurry with CO_2 increases SO_3^{2-} owing to the absorption of SO_2. The main chemical reactions by PCHP are shown in reactions (1)–(10) [19–32].

$$NO + O_3 \rightarrow NO_2 + O_2 \tag{1}$$

$$NO_2 + O_3 \rightarrow NO_3 + O_2 \tag{2}$$

$$SO_2 + O_3 \rightarrow SO_3 + O_2 \tag{3}$$

$$H_2O + SO_2 \rightarrow H_2SO_3 \tag{4}$$

$$2NO_2 + 4SO_3^{2-} \rightarrow N_2 + 4SO_4^{2-} \tag{5}$$

$$O_2 + 2SO_3^{2-} \rightarrow 2SO_4^{2-} \tag{6}$$

$$CaCO_3 + SO_2 \rightarrow CaSO_3 + CO_2 \tag{7}$$

$$CaCO_3 + CO_2 + H_2O \rightarrow Ca^{2+} + 2HCO_3^- \tag{8}$$

$$SO_2 + HCO_3^- \rightarrow HSO_3^- + CO_2 \tag{9}$$

$$HSO_3^- \rightarrow H^+ + SO_3^{2-} \tag{10}$$

3. Experimental

3.1 O_3 injection and absorption towers

Fig. 2 shows a schematic diagram of the O_3 injection and absorption towers. The O_3 injection tower was a cylindrical vessel made of SUS304 with an inner diameter of 56 mm and height of 980 mm. The z-axis was set in the vertical direction (upward: +) of the O_3 injection tower and $z = 0$ mm was set at the inlet of the simulated flue gas.
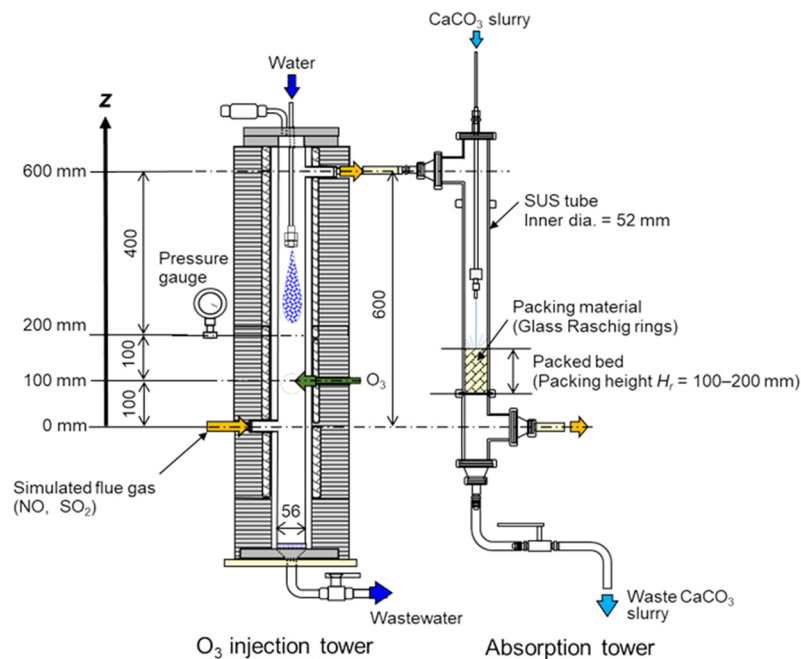

Fig. 2. Schematic diagram of the O_3 injection and absorption towers.

3

A 420 mm long heater (Eikou Electric Co., Ltd.: Voltage 100 V, Power 500 W) was installed on the upper wall of the O_3 injection tower, and a 400 mm long heater (Eikou Electric Co., Ltd.: Voltage 100 V, Power 450 W) was installed in the lower section. In the previous study [33], the effect of gas temperature on NO oxidation by O_3 was not observed under 100 °C. Therefore, the O_3 injection tower was not heated, resulting in the gas temperature of approximately 20. At $z = 100$ mm, the tip of the O_3 injection tube was placed at the center of the reactor, and O_3 was injected in a counterflow direction to the simulated flue gas flow. A Poppett check valve (SS-6C-25, Swagelok Company; cracking pressure of 0.18 MPa) was installed at the top to prevent pressurization inside the tower. The gas temperature was measured using thermocouples installed at $z = 0$, 100, 200, and 600 mm. The absorption tower has an inner diameter of 52 mm and a total length of 916 mm. The length from the inlet to the outlet of the absorption tower was 600 mm, which was the same as that of the O_3 injection tower. In an actual plant, a $CaCO_3$ slurry is sprayed using a spray nozzle; however, it is difficult to use a spray nozzle in laboratory-scale experiments due to the clogging of spray holes. Therefore, $CaCO_3$ slurry was sprayed from the top of the absorption tower using a 1/8-inch SUS tube and a rectification cap. In addition, Glass Raschig rings (FC-4, Asahi Glassplant Inc.: borosilicate glass, φ4 mm × 5 mm) were used as packing material. The porosity of the packed bed is approximately 50%. The sprayed $CaCO_3$ slurry collided with the packed bed and diffuse the $CaCO_3$ slurry into the packed bed, thereby promoting gas-liquid contact.

3.2 Experimental setup overview

A schematic of the experimental apparatus used in this study is shown in Fig. 3. The experimental apparatus, consisted of a simulated flue gas flow, O_3 flow, water spray flow, and lime slurry flow, and treats NO_x and SO_2 in the simulated flue gas using the combination of O_3 injection and absorption towers. A dust removal tower was not prepared in this study because the simulated exhaust did not contain dust. However, Some of NO_x and SO_2 is absorbed by water spray in the dust removal tower in the actual apparatus. Mass flow controllers (SFC280E, Hitachi Metals, Ltd.) were used to adjust the flow rate and concentration of N_2-based NO (NO = 200 ppm), N_2-based SO_2 (SO_2 = 2000 ppm), synthetic air (O_2 = 21%, N_2 = 79%), and a CO_2 cylinder (99.5%). The mixed gas was introduced into the lower part of the O_3 injection tower, where the flue gas flowed
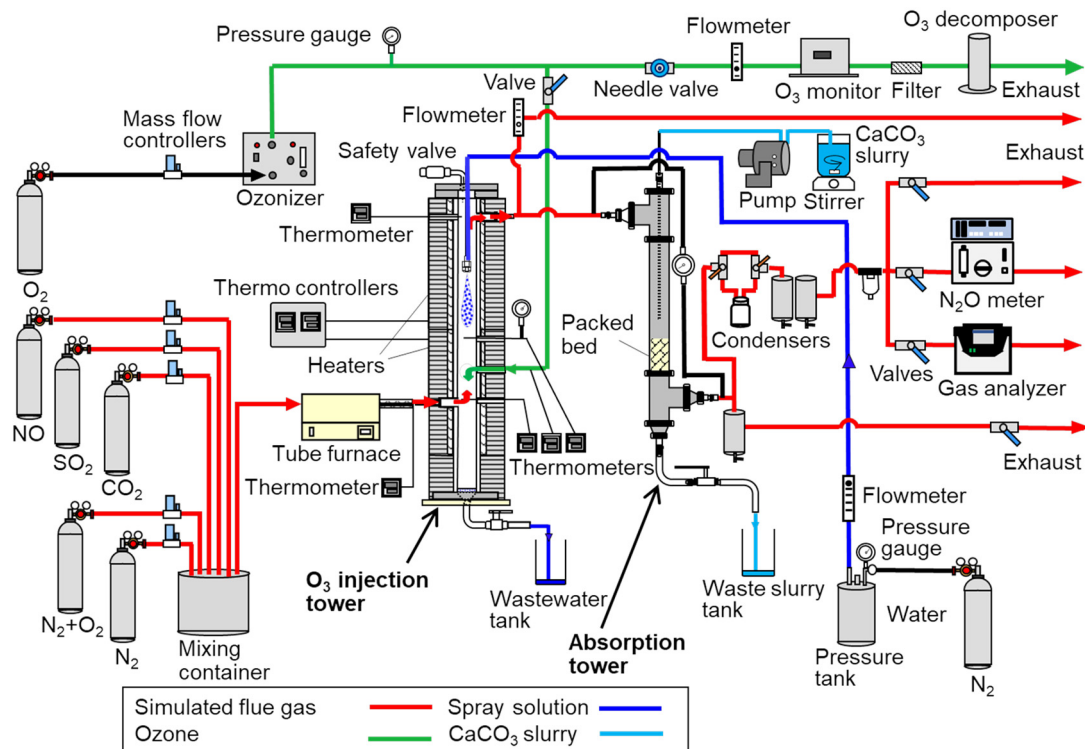

Fig. 3. Schematic diagram of the experimental setup.

upward from the bottom to the top and reacted with the O_3 in the cooling water spray area. O_3 was generated using a surface discharge-type ozonizer (OZS-OP60-12V, Masuda Research Inc.). The concentration of the O_3 generated was measured using an ozone monitor (EG-610, Ebara Jitsugyo Co., Ltd.), and the O_3 flow rate was adjusted using a flow meter before injection into the O_3 injection tower. Water in a stainless steel pressurized tank (TM18SRV, UNICONTROLS Co., Ltd.: 18 L) up to 0.45 MPa using an N_2 cylinder, and pumped to the top of the O_3 injection tower and sprayed from a one-fluid nozzle (UNIJET TIP-130783 TN SS0.11, Spraying Systems Co., Japan: full-cone type, spray angle 20º). The spray flow rate was set to 10 mL min^{-1} (standard temperature and pressure) using a flow meter (RK1250 SERIES, KOFLOC Corp.). The sprayed water that did not evaporate was discharged from the bottom of the O_3 injection tower through the valve. Following this treatment, the flue gas was discharged from the top of the O_3 injection tower and introduced at the top of the absorption tower. In the absorption tower, the flue gas flows downward from the top to the bottom and reacts with the $CaCO_3$ slurry. The $CaCO_3$ slurry was stirred using a magnetic stirrer (CT-3A, AS ONE Corporation), pumped using a tube pump (ST-1N, ELEPON E.C.A.P. Corporation: 72 mL min^{-1}), and sprayed from the top of the absorption tower. The $CaCO_3$ slurry absorbed SO_2 and NO_2 from the flue gas and was stored at the bottom of the absorption tower. Consequently, the flue gas was discharged from the bottom of the absorption tower. The concentrations of NO, NO_x, O_2, SO_2, and N_2O were then measured using a gas analyzer (PG-350, chemiluminescence analyzer for NO and NO_x, paramagnetic analyzer for O_2, non-dispersive infrared absorption analyzer for SO_2, Horiba, Ltd.) and an N_2O analyzer (VIA-510, non-dispersive infrared absorption, Horiba, Ltd.) before the exhaust.

3.3 NO oxidation by O_3 injection

To evaluate the NO oxidation performance in the presence of low concentrations of NO and high concentrations of SO_2, NO oxidation experiments were conducted using an O_3 injection tower. The experiments were conducted in two patterns: with and without water spraying. Without water spraying, the simulated flue gas was used for the following conditions: an initial NO concentration = 15 ppm, an initial SO_2 concentration = 150, 300, 450, and 690 ppm (SO_2/NO = 10, 20, 30, and 46), O_2 concentration = 6%, a simulated flue gas flow rate flowing in O_3 injection tower Q_1 = 10 L min^{-1}, O_2 flow rate = 0.20 L min^{-1}, O_3 concentration = 15 ppm after mixing. The O_3 injection into the O_3 injection tower began 5 min after the start of the experiment, and the experiment continued for a total of 10 min. The NO, NO_x, SO_2, and N_2O concentrations were measured every 5 min. For water spraying, the simulated flue gas was mixed at an initial NO concentration of 15 ppm, initial SO_2 concentrations of 0, 300, 450, and 690 ppm (SO_2/NO = 0, 20, 30, and 46), O_2 concentration = 6%, Q_1 = 10 L min^{-1}, and O_2 flow rate = 0.20 L min^{-1}, O_3 concentration = 1.6 g m^{-3}, and O_3 concentration = 15 ppm after mixing. The water spray flow rate q_1 was set to 7.0 m L min^{-1}. Water was sprayed into the O_3 injection tower 5 min after the start of the experiment, and the O_3 injection began 10 min later. Measurements were conducted for 20 min. The NO, NO_x, SO_2, and N_2O concentrations were measured every 5 min.

3.4 Simultaneous removal of NO_x and SO_2 using $CaCO_3$ slurry

The simultaneous removal of NO_x and SO_2 was evaluated by combining O_3 injection under water-spray conditions in the O_3 injection tower with $CaCO_3$ slurry injection in the absorption tower, assuming that the PCHP was installed between the dust removal and absorption towers in a coal-fired power plant. The simulated flue gas was used for the following conditions: the initial NO concentration = 15 ppm, the initial SO_2 concentration = 690 ppm (SO_2/NO = 46), O_2 concentration = 6%, Q_1 = 10 L min^{-1}, O_2 flow rate = 0.20 L min^{-1}, O_3 concentration = 1.6 g m^{-3}, and O_3 concentration after mixing = 15 ppm. q_1 was set to 7.0 mL/min. The $CaCO_3$ slurry spray flow rate, q_2, was set to 36–72 m L min^{-1}, and the $CaCO_3$ slurry concentrations were 10% and 30%. Experiments were also conducted by varying the residence time in the packed bed of the absorption tower, by varying the simulated flue gas flow rate in the absorption tower Q_2 = 3, 5, and 10 L min^{-1} and packing heights H_r = 100, 200, and 250 mm. The equation for residence time T_r (s) is as follows:

$$T_r = \frac{\alpha \pi H_r D_2^2}{4 Q_2} \tag{11}$$

where α (-) represents the porosity of the packed bed, D_2 denotes the inner diameter of the absorption tower. Water spraying on the O_3 injection tower was started 5 min after the start of the experiment, and O_3 injection

was started 10 min later. In addition, the CaCO$_3$ slurry was sprayed into the absorption tower 20 min after the start of the experiment. Measurements were conducted for 85 min. The NO, NO$_x$, SO$_2$, and N$_2$O concentrations were measured every 5 min.

For the low-concentration NO treatment, the O$_3$ concentration after injection was also low, and thus susceptible to oxidation inhibition by the water spray. Therefore, experiments were conducted by varying the O$_3$ concentration to improve NO$_x$ removal efficiency. Moreover, experiments using simulated flue gas containing 13% CO$_2$ were conducted because flue gas from a thermal power plant contains approximately 13% CO$_2$. The initial NO and SO$_2$ concentrations were 15 ppm and 690 ppm, respectively (SO$_2$/NO = 46). The O$_2$ and CO$_2$ concentration are 6% and 13%, respectively. The simulated flue gas flow rate in the O$_3$ injection tower was set to 10 L min^{-1}. The O$_2$ flow rate is 0.20 L min^{-1}, O$_3$ concentration is 1.6–2.4 g m^{-3} (15–23 ppm after mixing). The water spray flow rate is 7.0 m L min^{-1}, CaCO$_3$ slurry spray flow rate is 36 m L min^{-1}, CaCO$_3$ slurry concentration = 30%, the simulated flue gas flow rate flowing in the absorption tower is 3 L min^{-1}, and the packing height is 250 mm. Water spraying on the O$_3$ injection tower was started 5 min after the start of the experiment, and the O$_3$ injection was started 10 min later. In addition, the spraying of the CaCO$_3$ slurry into the absorption tower started 20 min after the start of the experiment. Measurements were conducted for 85 min, and NO, NO$_x$, SO$_2$, and N$_2$O concentrations were measured every 5 min.

4. Results and discussion

4.1 NO oxidation by O$_3$ injection

Fig. 4 shows the NO, NO$_x$, N$_2$O, and SO$_2$ concentrations in the NO oxidation experiment at SO$_2$/NO = 30. Fig. 4 (a) shows the results of O$_3$ injection only, and Fig. 4 (b) shows the results of O$_3$ injection and water spraying. Fig. 4 (a) shows that NO concentration decreased by 13.4 ppm and NO$_x$ concentration decreased by 1.6 ppm before and after O$_3$ injection, while SO$_2$ concentration did not change. The O$_3$ injection was effective for NO oxidation, whereas water spraying was effective for SO$_2$ removal. Fig. 5 shows the effect of SO$_2$ concentration on ΔNO/O$_3$, NO$_x$ removal efficiency, and SO$_2$ removal efficiency in the NO oxidation experiment. Fig. 5 (a) shows the results of O$_3$ injection only, and Fig. 5 (b) shows the results of O$_3$ injection and water spraying. Fig. 5 (b) shows that the initial SO$_2$ concentration did not affect NO oxidation, even when O$_3$ injection and water spraying were performed. However, the NO oxidation efficiency was lower than that of O$_3$ injection alone. This was due to the reaction between water and O$_3$. Under SO$_2$/NO = 46, which is the flue gas condition of the actual plant, the NO oxidation efficiency was 70% on average, and SO$_2$ was removed by about 10% under the influence of sprayed water; the reaction of SO$_2$ with water produced SO$_3^{2-}$. The NO$_2$ produced by NO and O$_3$ is absorbed more rapidly as the SO$_3^{2-}$ concentration increases, which may explain the increase in NO$_x$ removal efficiency as the SO$_2$ concentration increases [34]. The absorption is accelerated; thus, the NO$_x$ removal efficiency is considered to increase with increasing SO$_2$ concentration [34].
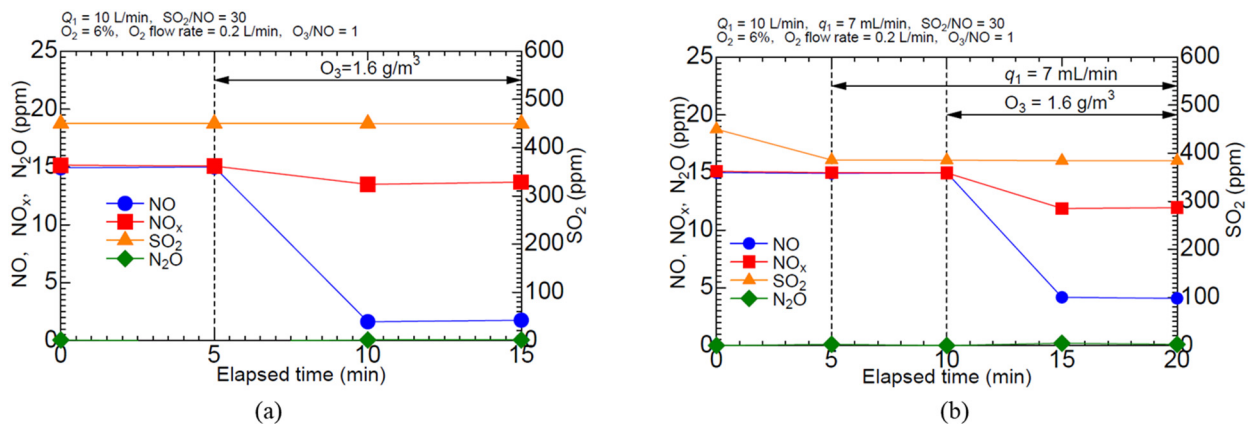

Fig. 4. Gas concentration when the O$_3$ injection tower was used under the condition of SO$_2$/NO = 30 (a)Without water spray, (b)With water spray.
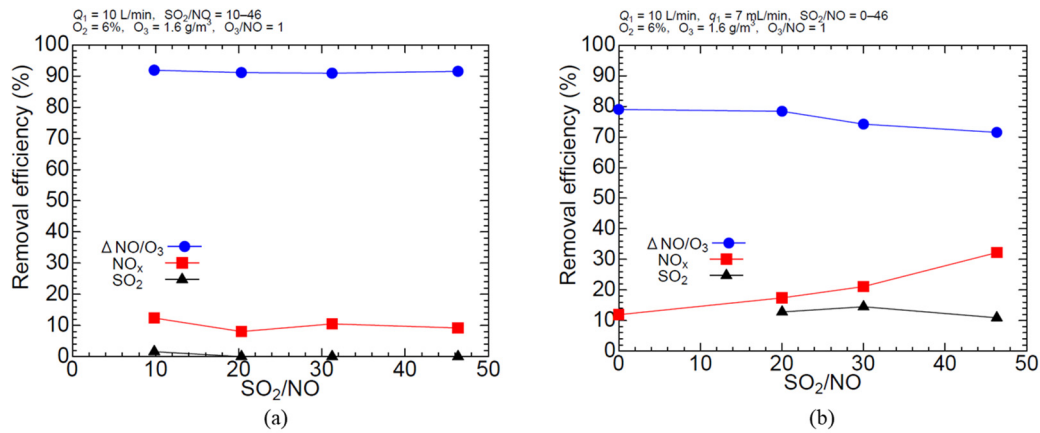
Fig. 5. Δ NO/O_3 and the removal efficiencies of NO_x and SO_2 when O_3 injection was conducted (a)Without water spray, (b)With water spray.

4.2 Simultaneous removal of NO$_x$ and SO$_2$ by CaCO$_3$ slurry

Experiments were conducted on NO oxidation by O_3 injection and the simultaneous removal of NO_x and SO_2 by a CaCO$_3$ slurry under water-spraying conditions using both O_3 injection and absorption towers. In actual equipment, the CaCO$_3$ slurry is sprayed using a spray nozzle, whereas at the laboratory scale, the spray nozzle is clogged and cannot be sprayed. Therefore, we evaluated the denitrification performance under conditions in which the packing material was used to promote gas-liquid contact and achieve a desulfurization efficiency close to that of an actual plant. In this experiment, the residence time in the packed bed of the absorption tower varied according to the packing height and flue-gas flow rate in the absorption tower.
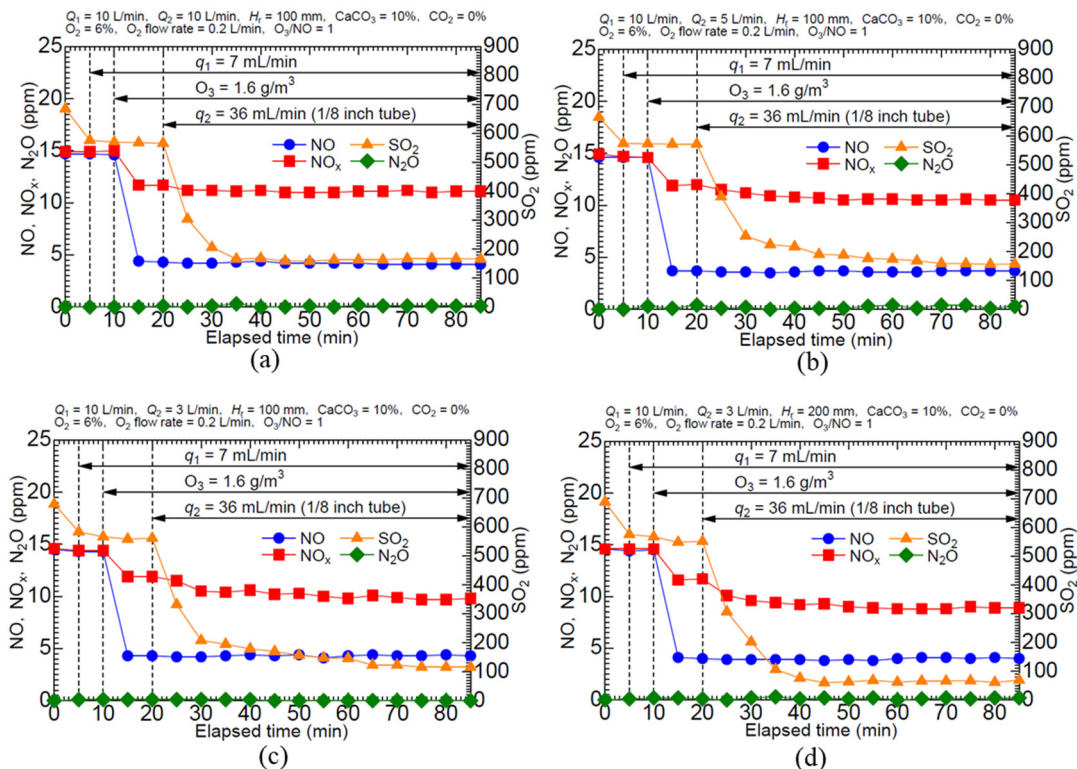

Fig. 6. Gas concentrations when the O_3 injection and absorption towers were used under the condition of SO$_2$/NO=46 and CaCO$_3$ = 30% for various flue gas flow rates and packing heights, with residence time of: (a) 2.4 s, (b) 4.8 s, (c) 8 s and (d) 16 s.
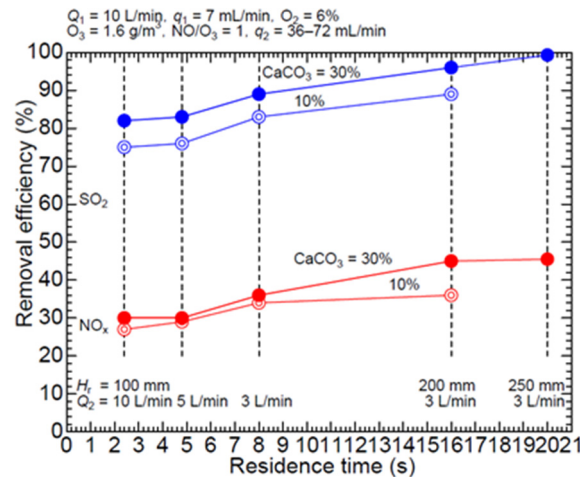
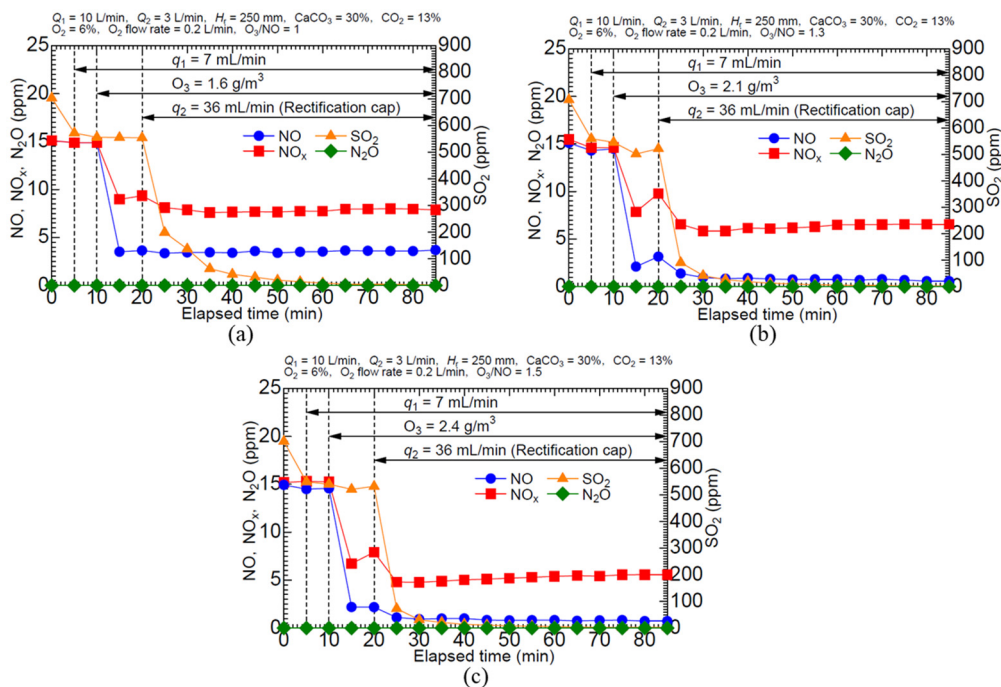**Fig. 7.** NO_x and SO_2 removal efficiencies when the O_3 injection and absorption towers were used.

Fig. 8. Gas concentrations when the O_3 injection and absorption towers were used under the condition of $SO_2/NO=46$, $CaCO_3 = 30\%$, $CO_2 = 13\%$, residence time 20 s and O_3 concentration (a) 1, (b) 1.3 and (c) 1.5.

Fig. 6 shows the NO, NO_x, N_2O, and SO_2 concentrations at $SO_2/NO = 46$ and $CaCO_3$ slurry concentration of 10% for residence times of (a) 2.4 s, (b) 4.8 s, (c) 8 s, and (d) 16 s in packed bed of the absorption tower. Water spray, O_3 injection, and $CaCO_3$ slurry injection were started 5, 10, and 20 min after the start of the experiment. The NO_x and SO_2 concentrations decreased before and after $CaCO_3$ slurry injection. This is because the absorption of NO_2 was enhanced by the SO_3^{2-} produced by the reaction of SO_2 with the $CaCO_3$ slurry [34]. Fig. 7 shows the removal efficiencies of SO_2 and NO_x as a function of residence time in the packed bed of the absorption tower. The NO_x and SO_2 removal efficiencies increased with the residence time. At a residence time of 20 s, a SO_2 removal efficiency of 99% was achieved, which is equivalent to that of an actual plant. The NO_x and SO_2 removal efficiencies increased with increasing $CaCO_3$ concentrations. This was due to the increase in $CaSO_3$ produced as the $CaCO_3$ concentration increased [29]. SO_3^{2-}, which is effective for NO_x removal, is formed by the reaction of SO_2 with slurry. In previous studies, SO_3^{2-} was oxidized by O_2 in flue gas when SO_2 was absorbed into water in the presence of SO_2 and O_2. This reaction occurs strongly when the pH of the absorbent is approximately 7 and the sulfite produced is almost zero. Conversely, the highest amount of sulfite is produced when the pH is approximately 4 [32]. In this study, the pH of the $CaCO_3$ slurry was approximately 7, regardless of the residence time; therefore, reaction (6) took priority over reaction (5),

and NO_x removal was inhibited. For further NO_x removal, it is necessary to decrease the pH of the $CaCO_3$ slurry and increase the amount of SO_3^{2-} produced. The actual flue gas from a thermal power plant contains approximately 13% CO_2, and the pH of the $CaCO_3$ slurry is reduced by absorbing CO_2. The $Ca(HCO_3)_2$ generated by CO_2 absorption has a higher solubility in water than $CaCO_3$. Therefore, the addition of CO_2 to the simulated flue gas brings the gas conditions closer to those of an actual plant and promotes NO_x and SO_x removal through gas-liquid contact with the slurry. In addition, because NO does not react with $CaCO_3$ slurry, the NO oxidation efficiency must be increased to improve the NO_x removal efficiency. Fig. 8 shows the NO, NO_x, N_2O, and SO_2 at $SO_2/NO = 46$, $CaCO_3$ slurry concentration of 30%, and residence time of 20 s in the absorption tower with (a) $O_3/NO = 1$, (b) 1.3, and (c) 1.5. Water spraying, O_3 injection, and $CaCO_3$ slurry injection were initiated at 5, 10, and 20 min after the start of the experiment. The results show that CO_2 is effective in increasing NO_x removal while increasing O_3 concentration is effective in increasing NO oxidation and NO_x removal.
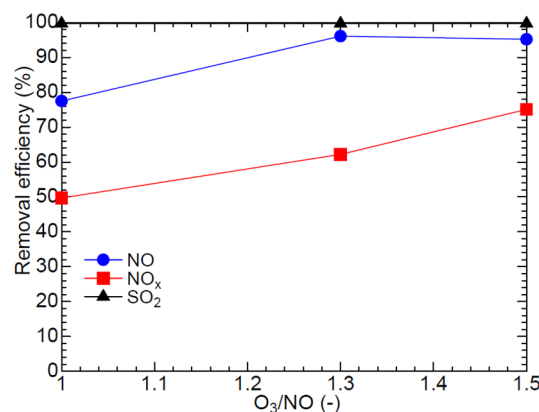

Fig. 9. NO oxidation rate and NO_x and SO_2 removal efficiencies when the O_3 injection and absorption towers were used.

Fig. 9 shows the NO oxidation efficiency and SO_2 and NO_x removal efficiencies versus O_3/NO. The NO_x removal efficiencies were 50, 62, and 75 for $O_3/NO = 1$, 1.3, and 1.5, respectively. Under the present experimental conditions, the NO oxidation efficiency was 96%, with the highest NO oxidation efficiency observed at O_3/NO ratios greater than 1.3. This was due to the formation of NO_3 by Reaction (2). Although the electric power required to generate O_3 is high, the NO_x removal efficiency can be increased without modifying the equipment, and the system can respond to changes in NO_x emissions owing to changes in the amount of electricity generated by thermal power plants. Therefore, PCHP can be retrofitted to thermal power plant flue-gas treatment facilities to comply with strict NO_x emission regulations.

4. Conclusion

The simulated flue gas containing high-concentration SO_2 and low-concentrations NO was subjected to NO oxidation using an O_3 injection tower and simultaneous removal of NO_x and SO_x using an O_3 injection tower and an absorption tower with $CaCO_3$ slurry, assuming that PCHP would be introduced into the thermal power plant flue gas treatment. The main results are summarized as follows.

(1) Experiments on NO oxidation by O_3 injection into flue gas containing low-concentration NO and high-concentration SO_2 in an O_3 injection tower showed that O_3 sufficiently oxidized NO without reacting with SO_2. O_3 injection resulted in NO oxidation of approximately 90% without water spraying and approximately 70% with water spraying, regardless of the initial SO_2 concentration. The NO oxidation efficiency with water spray was lower than that without water spray because O_3 was absorbed by water. Without water spray, the NO_x removal efficiency was approximately 10%. This is because some of the injected O_3 reacts with NO_2 at $O_3/NO = 1$. However, with water spray, the NO_x removal efficiency increased as the SO_2 concentration increased, and some of the SO_2 was absorbed by the water and decreased by approximately 10%, suggesting that SO_3^{2-} corresponding to the decrease was generated, and NO_2 was reduced to N_2.

(2) The simultaneous removal of NO_x and SO_2 was performed using the O_3 injection and absorption towers together and by varying the residence time in the packed bed of the absorption tower to make the reaction time closer to that of the actual system. A SO_2 removal efficiency of 99% was achieved when the residence time was 20 s, which was the same as that of the actual plant. The NO_x and SO_2 removal efficiencies increased with increasing $CaCO_3$ concentrations. This was due to an increase in the amount of $CaSO_3$ produced as the $CaCO_3$ concentration increased.

(3) To approximate the gas conditions to those of an actual plant and to accelerate NO_x and SO_x removal by gas-liquid contact with the slurry, experiments were conducted by adding 13% CO_2 to the simulated flue gas and varying the O_3 concentration. As O_3/NO increased from 1 to 1.3, the NO oxidation efficiency increased from 78% to 96%. At $O_3/NO = 1.5$, the NO oxidation efficiency was 95%, which is almost the same as that at $O_3/NO = 1.3$. The NO_x removal efficiencies were 50, 62, and 75 for $O_3/NO = 1$, 1.3, and 1.5, respectively. Under the present experimental conditions, the NO oxidation efficiency was 96%, with the highest NO oxidation efficiency observed at O_3/NO ratios greater than 1.3. Although the power required to generate O_3 is high, the NO_x removal efficiency can be increased without changing the equipment, and it is possible to respond to changes in NO_x emissions due to changes in the amount of electricity generated by thermal power plants. Therefore, PCHP can be retrofitted to thermal power plant flue-gas treatment facilities to comply with strict NO_x emission regulations.

Acknowledgment

References

[1] Zou P., Chen Q., Yu Y., Xia Q., and Kang C., Electricity markets evolution with the changing generation mix: An empirical analysis based on China 2050 high renewable energy penetration roadmap, *Appl. Energy*, Vol. 185, pp. 56–67, 2017.

[2] Gómez A., Zubizarreta J., Dopazo C., and Fueyo N., Spanish energy roadmap to 2020: Socioeconomic implications of renewable targets, *Energy*, Vol. 36 (4), pp. 1973–1985, 2011.

[3] Hassan Q., Viktor P., Al-Musawi T.J, Ali B.M., Algburi S., Alzoubi H.M., Al-Jiboory A.K., Sameen A.Z., Salman H.M., and Jaszczur M., The renewable energy role in the global energy transformations, *Renew. Energy Focus*, Vol. 48, 100545, 2024.

[4] Agency for Natural Resources and Energy, The 6th Strategic Energy Plan, Available: https://www.enecho.meti.go.jp/category/others/basic_plan/pdf/strategic_energy_plan.pdf, 2021.

[5] Takao K., Hara S., Kiriyama T., Hashimoto A., Kaneko S., Izumi S., and Sakai S., Analysis on demand and supply operation in electric power system under high renewable penetration using optimal power generation mix model, *Trans. JSME*, Vol. 80 (820), TEP0366, 2014. (in Japanese)

[6] Sun C., Liu H., Chen W., Chen D., Yu S., Liu A., Dong L., and Feng S., Insights into the Sm/Zr co-doping effects on N_2 selectivity and SO_2 resistance of a MnO_x-TiO_2 catalyst for the NH_3-SCR reaction, *Chem. Eng. J.,* Vol. 347, pp 27–40, 2018.

[7] Miessner H., Francke K.P., Rudolph R., and Hammer Th., NO_x removal in excess oxygen by plasma-enhanced selective catalytic reduction, *Catal. Today*, Vol. 75(1–4), pp 325–330, 2002.

[8] Kang M., Park E.D., Kim J.M., and Yie J.E., Manganese oxide catalysts for NO_x reduction with NH_3 at low temperatures, *Appl. Catal. A*, Vol. 327 (2), pp. 261–269, 2007.

[9] Forzatti P., Present status and perspectives in de-NO_x SCR catalysis, *Appl. Catal. A*, Vol. 222 (1–2), pp 221–236, 2001.

[10] Zhao S., Peng J., Ge R., Wu S., Zeng K., Huang H., Yang K., and Sun Z., Research progress on selective catalytic reduction (SCR) catalysts for NO_x removal from coal-fired flue gas, *Fuel Process. Technol.*, Vol. 236, 107432, 2022.

[11] Guan B., Zhan R., Lin H., and Huang Z., Review of state of the art technologies of selective catalytic reduction of NO_x from diesel engine exhaust, *Appl. Therm. Eng.*, Vol. 66 (1–2), pp. 395–414, 2014.

[12] Shuangchen M., Jin C., Gongda C., Weijing Y., and Sijie Z., Research on desulfurization wastewater evaporation: Present and future perspectives, *Renew. Sustain. Energy Rev*., Vol. 58, pp. 1143–1151, 2016.

[13] Lee S., Kim Y., and Hong S., Treatment of industrial wastewater produced by desulfurization process in a coal-fired power plant via FO-MD hybrid process, *Chemosphere*, Vol. 210, pp. 44–51, 2018.

[14] Aunela-Tapola L., Hatanpää E., Hoffren H., Laitinen T., Larjava K., Rasila P., and Tolvanen M., A study of trace element behaviour in two modern coal-fired power plants: II. Trace element balances in two plants equipped with semi-dry flue gas desulphurization facilities, *Fuel Process. Technol.*, Vol. 55 (1), pp. 13–34, 1998.

[15] Jolibois J., Takashima K., and Mizuno A., Application of a non-thermal surface plasma discharge in wet condition for gas exhaust treatment: NO_x removal, *J. Electeostat.*, Vol. 70 (3), pp. 300–308, 2012.

[16] Ighigeanu D., Martin D., Zissulescu E., Macarie R., Oproiu C., Cirstea E., Iovu H., Calinescu I., and Iacob N., SO_2 and NO_x removal by electron beam and electrical discharge induced non-thermal plasmas, *Vacuum*, Vol. 77 (4), pp. 493–500, 2005.

[17] Ma S., Zhao Y., Yang J., Zhang S., Zhang J., and Zheng C., Research progress of pollutants removal from coal-fired flue gas using non-thermal plasma, *Renew. Sustain. Energy Rev.*, Vol. 67, pp. 791–810, 2017.

[18] Chae J.O., Non-thermal plasma for diesel exhaust treatment, *J. Electrostat.*, Vol. 57 (3–4), pp. 251–262, 2003.

[19] Wang Z., Zhou J., Zhu Y., Wen Z., Liu J., and Cen K., Simultaneous removal of NO_x, SO_2 and Hg in nitrogen flow in a narrow reactor by ozone injection: experimental results, *Fuel Process. Technol.*, Vol. 88 (8), pp. 817–823, 2007.

[20] Obradović B.M., Sretenović G.B., and Kuraica M.M., A dual-use of DBD plasma for simultaneous NO_x and SO_2 removal from coal-combustion flue gas, *J. Hazard. Mater.*, Vol. 185 (2–3), pp. 1280–1286, 2011.

[21] Chen G., Gao J., Gao J., Du Q., Fu X., Yin Y., and Qin Y., Simultaneous removal of SO_2 and NO_x by calcium hydroxide at low temperature: Effect of SO_2 absorption on NO_2 removal, *Ind. Eng. Chem. Res.*, Vol. 49 (23), pp. 12140–12147, 2010.

[22] Mok Y.S., and Lee H.J., Removal of sulfur dioxide and nitrogen oxides by using ozone injection and absorption–reduction technique, *Fuel Process. Technol.*, Vol. 87 (7), pp. 591–597, 2006.

[23] Yamasaki H., Mizuguchi H., Maeda K., Fujishima H., Kuroki T., Yamamoto H., and Okubo M., Performance evaluation of semi-dry flue gas desulfurization and denitration from flue gas of a glass melt using nonthermal plasma combined process, *Mech. Eng. J.*, Vol. 8 (2), 20–00519, 2021.

[24] Yamamoto H., Kuroki T., Fujishima H., Yamamoto Y., and Yoshida K., Pilot-scale exhaust gas treatment for a glass manufacturing system using a plasma combined semi-dry chemical process, *IEEE Trans. Ind. Applicat.*, Vol. 53 (2), pp. 1416–1423, 2017.

[25] Fukuda Y., Kuroki T., Nishioka R., Fujishima H., Yamasaki H., Yamamoto H., and Okubo M., Performance improvement in semi-dry ozone injection NO_x and SO_x removal process for a glass furnace flue gas, *Ozone Sci. Eng.* Vol. 44(5), pp. 453–463, 2022.

[26] Atkinson R., Baulch D.L., Cox R.A., Crowley J.N., Hampson R.F., Hynes R.G., Jenkin M.E., Rossi M.J., and Troe J., Evaluated kinetic and photochemical data for atmospheric chemistry: Volume I – gas phase reactions of O_x, HO_x, NO_x and SO_x species, *Atm. Chem. Phys.*, Vol. 4 (6), pp. 1461–1738, 2004.

[27] National Institute for Standards and Technology (NIST), Chemical kinetics database, https://kinetics.nist.gov/kinetics/Detail?id=1997DEM/SAN1-266:385, 6 October 2022.

[28] Dentener F.J., and Crutzen P.J., Reaction of N_2O_5 on tropospheric aerosols impact on the global distributions of NO_x, O_3, and OH, *J. Geophys. Res.*, Vol. 98 (D4), pp. 7149–7163, 1993.

[29] Wang Z., Zhang X., Zhou Z., Chen W.Y., Zhou J., and Cen K., Effect of additive agents on the simultaneous absorption of NO_2 and SO_2 in the calcium sulfite slurry, *Energy Fuels*, Vol. 26 (9), pp. 5583–5589, 2012.

[30] Liu S.Y., and Xiao W.D., Modeling and simulation of bubbling SO_2 absorber with granular limestone slurry and an organic acid additive, *Chem. Eng. Technol.*, Vol. 29 (10), pp. 1167–1173, 2006.

[31] Santschi Ch., and Rossi M.J., Uptake of CO_2, SO_2, and HCl on calcite ($CaCO_3$) at 300 K: mechanism and the role of adsorbed water, *J. Phys. Chem. A*, Vol. 110 (21), pp. 6789–6802, 2006.

[32] Tang N., Liu Y., Wang H., Xiao L., and Wu Z., Enhanced absorption process of NO_2 in $CaSO_3$ slurry by the addition of $MgSO_4$, *Chem. Eng. J.*, Vol. 160 (1), pp. 145–149, 2010.

[33] Inoue J., Itagaki T., Tanaka T., Kuroki T., Yamasaki H., Yamamoto H., Hattori M., and Okubo M., Low concentration NO_x removal using plasma-chemical hybrid process combined with limestone-gypsum desulfurization, *Proc. of 17th Int. Conf. Electrostatic Precipitation*, Kyoto, 2024.

[34] Ninomiya K., Imaura M., and Kono H., Absorption reactions of NO-NO_2 gas mixtures with ammonium sulfite solutions, *NIPPON KAGAKU KAISHI*, Vol. 1981(12), pp. 1846–1854, 1981. (in Japanese)